Analysis of Defective Interconnections of the 13 kA LHC Superconducting Bus Bars

Pier Paolo Granieri, Marco Casali, Marco Bianchi, Marco Breschi, Luca Bottura, and Gerard Willering

***Abstract*—The interconnections between Large Hadron Collider (LHC) main dipole and quadrupole magnets are made of soldered joints of two superconducting cables stabilized by a copper bus bar. The 2008 incident revealed the possible presence of defects in the interconnections of the 13 kA circuits that could lead to unprotected resistive transitions. Since then thorough experimental and numerical investigations were undertaken to determine the safe operating conditions for the LHC.**

This paper reports the analysis of experimental tests reproducing defective interconnections between main quadrupole magnets. A thermo-electromagnetic model was developed taking into account the complicated sample geometry. Close attention was paid to the physical description of the heat transfer towards helium, one of the main unknown parameters. The simulation results are reported in comparison with the measurements in case of static He I cooling bath. The outcome of this study constitutes a useful input to improve the stability assessment of the 13 kA bus bars interconnections.

***Index Terms*—Accelerator magnets, interconnection, LHC, superconducting bus bar.**

I. Introduction

THE 2008 incident of the CERN particle accelerator occurred in an interconnection (IC) between the main magnets of the Large Hadron Collider (LHC) ring [1]. This event triggered systematic investigations of the 13 kA superconducting (SC) bus bars. Electrical resistance measurements [2] as well as imaging techniques [3] allowed determining the presence of high-resistance joints in the machine, the largest of which were repaired. Their origin was identified to be the bad soldering, responsible for the lack of electrical contact between the SC cables and the bus bar copper stabilizer, as well as along the bus bar stabilizer itself. That results in a defect, which maximum expected length is approximately 50 mm, where the SC cable is not stabilized. Such defect can lead to an unprotected thermal runaway. This calls for caution and justifies the decision to limit operation below 11.8 kA. According to modeling of the IC stability [4], [5] that provided estimations of the maximum allowed operating current, the LHC is being exploited at half the energy during the first years, and will require consolidation actions to operate at full energy [6]. A tests campaign was carried out on instrumented IC samples featuring purposely built-in defects [7], in order to provide an experimental benchmark for the model and to study design improvements.

This paper reports on the analysis of the tests reproducing defective ICs in liquid helium. A coupled thermal and electromagnetic model was developed, focusing on the definition of local heat transfer coefficients between the components and the cooling helium bath. The importance of this parameter in the IC stability and quench propagation mechanisms was indeed highlighted in [5]. The description of the heat transfer coefficient in the bus bar region was addressed in [8] through the analysis of dedicated thermal measurements, whereas the heat exchange in the IC region still constitutes an unknown parameter. The numerical calculations are compared to the measured temperature and voltage traces, allowing to obtain a deeper insight of the physical mechanisms occurring in the IC.

Section II presents the main features of the experimental facility. In Section III the developed thermal and electromagnetic models are described, whereas Section IV reports the main results in comparison with the measurements.

II. Experimental Setup

The experimental measurements were performed in the FRESCA test station at CERN. The setup details and results are described in [7]. Several defective ICs of the main quadrupole type [9], [10] were tested, both in superfluid and liquid helium bath, in various operating conditions. The analyses of this paper refer to the tests at 4.3 K without external magnetic field of the sample 2B. This sample features a 35 mm long defect located on one side of the IC, corresponding to an additional resistance at 300 K of 42 $\mu\Omega$.

Fig. 1 shows a picture of the sample 2B (in one leg, together with sample 2A in the other leg), whereas in Fig. 2 a sketch of its longitudinal cross-section is given. The overlapping region of the SC cables is enclosed between the Cu stabilizer profiles constituting the IC. In the left joint between IC and bus bar the SnAg ensures the Cu stabilizer continuity, whereas a defect is simulated in the right joint thanks to polyimide layers around the SC cables and between IC and bus bar stabilizer. The void spaces inside IC and bus bar are filled by SnAg solder, except in correspondence to the IC ends. Thermofoil heaters were placed in contact with the IC (heater W) and the bus bar (heater M) stabilizer to start the normal zone, with additional polyimide foils below them to provide a better thermal insulation from the bath. The sample electrical insulation was made of $\sim$200 mm long U-shaped polyimide and VP-310 pieces for the IC [11], and of polyimide and ISOPREG wrappings for the bus bar [9].

Manuscript received September 13, 2011; accepted December 02, 2011. Date of publication December 20, 2011; date of current version May 24, 2012.

P. P. Granieri is with the Technology Department, CERN, Geneva, Switzerland, and also with the Swiss Federal Institute of Technology (EPFL), Particle Accelerator Physics Laboratory (LPAP), Lausanne, Switzerland (e-mail: Pier.Paolo.Granieri@cern.ch).

M. Casali, M. Bianchi, and M. Breschi are with the Department of Electrical Engineering (DIE), University of Bologna, Bologna, Italy.

L. Bottura and G. Willering are with the Technology Department, CERN, Geneva, Switzerland.

Digital Object Identifier 10.1109/TASC.2011.2180275

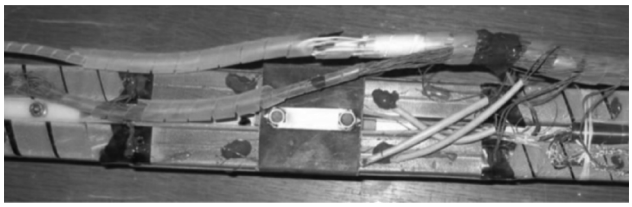

Fig. 1. Picture of the tested sample (top view).

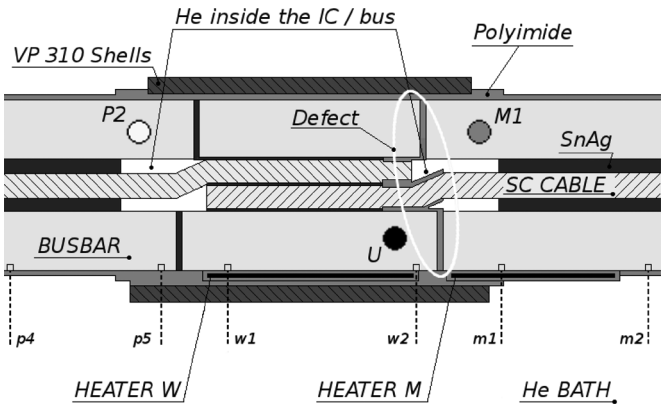

Fig. 2. Sketch of the longitudinal cross-section of the sample (side view).

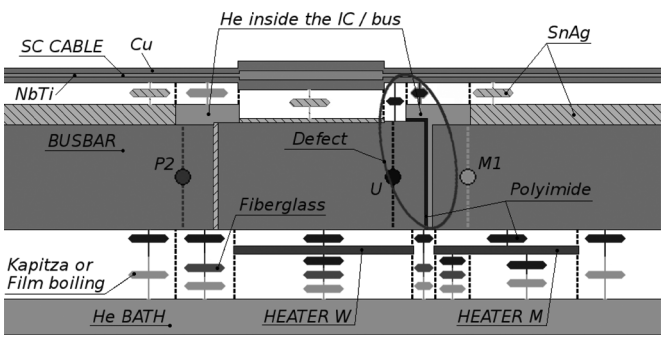

Fig. 3. Sketch of the thermal model developed for the numerical calculations.

The thermo-couple junctions $P2, U$ and $M1$ were located inside the left bus bar, IC and right bus bar Cu stabilizer, respectively. Voltage taps were soldered on top of the stabilizer: $p4$, $p5$, $w1$ and $w2$ on the left of the defect, $m1$ and $m2$ on its right.

III. Model Description

The present calculations are based on a coupled thermo-electromagnetic 1-D model of the sample [12]. The coupling is realized through temperature-dependent electrical properties of materials and the introduction in the thermal model of the Joule power calculated with the electromagnetic model.

A. Thermal Model

Fig. 3 describes the thermal model where the following elements are defined: SC cables (made of Nb-Ti and Cu), stabilizer (made of Cu and SnAg) and constantan heaters. The sample length of 1.7 m guarantees that the boundary conditions do not affect the 150 mm long IC region. The temperature, current and magnetic field dependence of the material properties are accounted for. In the cases reported in the paper the only considered magnetic field is the self-field.

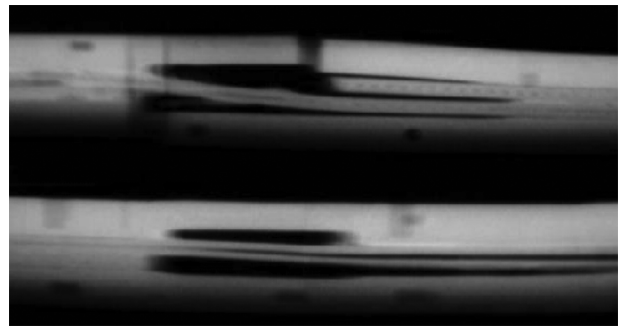

Fig. 4. Gamma ray picture of the defective side (above) and of the well soldered side (below) of the sample IC. The (black) void spaces inside the IC are not filled by SnAg.

The γ-ray picture of the two IC ends in Fig. 4 show that SnAg does not fill all the void spaces inside the IC and the bus bar. As it will be explained in Section IV-A, the tests without current can be reproduced if considering He filling these void spaces and undergoing the boiling transition.

The thermal resistances among the elements are defined by solid conduction through polyimide and SnAg layers. The heat transfer coefficient between the Cu stabilizer and the 4.3 K He bath changes from the bus bar to the IC region. For the bus bar region the steady-state measured values reported in [8] are used. Depending on the heat flux, they were modeled as the series of either Kapitza and polyimide thermal resistance, or polyimide and a film boiling layer thermal resistance. The latter is considered to blanket the polyimide surface. For the IC region the heat transfer coefficient below a stabilizer temperature of 6.5 K is given by solid conduction through the polyimide and fiberglass (used to model VP310) layers. Above that temperature the thermally insulating film boiling layer is considered, described by a heat transfer coefficient of 250 $\mathrm{W/m^2\ K}$. The threshold temperature represents a rough model to describe film boiling formation in the IC. It is calculated from the heat flux at which, according to [8], film boiling formation occurs around the bus bar. As for the heat transfer from stabilizer and cables to the He filling the void spaces inside IC and bus bar, it was described by the Kapitza resistance Cu-He before the He vaporizes and by the film boiling heat transfer coefficient afterwards. A summary of the main geometric parameters of the model is reported in Table I.

B. Electromagnetic Model

The sample is modeled by two electrical elements, the SC cables and the stabilizer, corresponding to the above mentioned thermal ones. The defect causes the opening of the stabilizer circuit, hence the whole transport current is forced to flow through the non-stabilized SC cable. As a consequence large Joule power is generated inside the IC in case of a quench. In such case the temperature and voltage response of the model is very sensitive with respect to the parameters that drive the Joule effect inside the IC. The tuning of the thermal and electrical resistances between the Cu stabilizer and the SC cables was therefore necessary, to take into account the contact resistances in addition to the SnAg bulk heat and current transport properties [13]. The ratio of the tuned thermal and electrical conductivity yields a value of 3.5, which agrees with

TABLE 1
MAIN GEOMETRIC PARAMETERS OF THE MODEL

Cross-section:	SC Cables (IC - bus)	(mm^2)	38.5 - 19.2
	Stabilizer Cu (IC - bus)	(mm^2)	150.2 - 146.6
	He in IC ends (IC – bus)	(mm^2)	67.7 – 28.75
Length:	Sample	(mm)	1715
	Overlap between cables	(mm)	117
	Distance between IC ends	(mm)	150
	Defect	(mm)	35
Avg thickness:	Polyimide insulat. (IC - bus)	(μm)	208 – 296
	Fiberglass (IC)	(μm)	1332
	SnAg (IC - bus)	(μm)	291 – 781

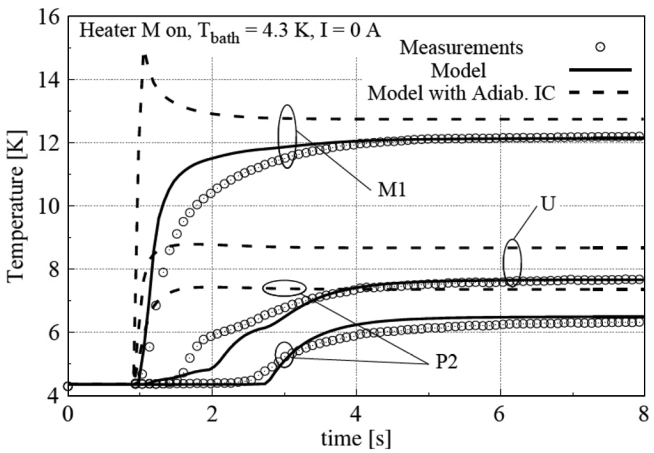

Fig. 5. Measured vs. calculated temperatures in case of no current and only heater M switched on. The developed model (solid lines) is compared to a simplified one assuming an adiabatic IC (dashed lines), i.e., no heat transfer to bath and no He filling the void spaces inside it.

the α coefficient included in the Wiedemann-Franz law in [14] to account for impure materials.

The Residual Resistivity Ratio (*RRR*) of the Cu components was set to the measured values, except the Cu cables *RRR* that was set to 130 instead of the measured 160 to reproduce the measured voltage traces. The values of the tuned parameters are kept constant throughout all the simulations.

IV. SIMULATION RESULTS

A. Tests Without Current

Fig. 5 reports measured and calculated temperatures for a heater calibration test: only heater M was turned on for 30 s with a power of 18 W, without any current flowing in the sample. The steady-state temperature, reached after few seconds, is higher for the sensor located below the heater M than for the sensors on the other side of the defect.

The calculations are performed using both a simplified model featuring an adiabatic IC and the complete model described in Section III-A. The simplified model, assuming no heat transfer

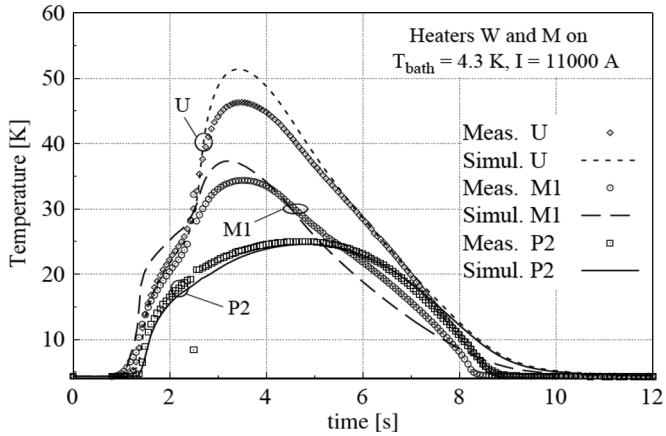

Fig. 6. Measured vs. calculated temperatures in case of 11 kA current and both heaters switched on.

towards the He bath and no He filling the void spaces inside IC and bus bar, does not catch the features of the measurements. The calculated steady-state temperatures are higher than the measured ones, the transient states are also very different and the measured time delays are not predicted. The complete model instead well simulates the test. The heat transfer through the IC insulation lowers the steady-state temperatures that are correct within 0.2 K. The He inside the IC and the bus bar allows reproducing the transient features and the initial time delays. It is worth noting that the changes of slope of the calculated curves, which reflect those of the measured ones, are associated to boiling of the He inside IC and bus bar. In particular the first change of slope of the calculated U curve occurring at 2 s is associated to the end of boiling of the He close to the defect. The second change of slope at 2.4 s corresponds to the start of boiling of the He located at the left IC extremity. The end of boiling of this He occurs at 2.7 s when the U curve features the last change of slope and the $P2$ sensor, located just on top of this He, starts heating up.

B. Tests With Current

In the tests with current the heat sources are both external and internal, respectively due to heaters M and W both turned on and to Joule heating in the resistive components. Figs. 6 and 7 report the time evolution of the three thermo-couple junctions and of four voltage traces, respectively, for a current of 11 kA. Two of the reported voltage traces are located on one side of the defect, $p4 - w2$ and $p5 - w1$, whereas $p4 - m2$ and $w2 - m1$ cross the defect zone.

The current is ramped up to the constant level of 11 kA and no voltage is detected in the first second, before the heaters are fired. The heat pulse of 15 W for heater M and 14 W for heater W lasts between 1 and 2.2 s. The voltages across the defect zone have a non-linear increase, even after the heaters are turned off, with a delay of 0.4 s after the beginning of the pulse. As soon as the threshold for switching off the power supply is reached, the current is shut down with a dump time of few hundreds of milliseconds and the sample recovers the superconducting state. It is worth noting that the voltage remains almost one order of magnitude lower in the left side of the IC with respect to the defect zone. This is due to the larger heat generation and the

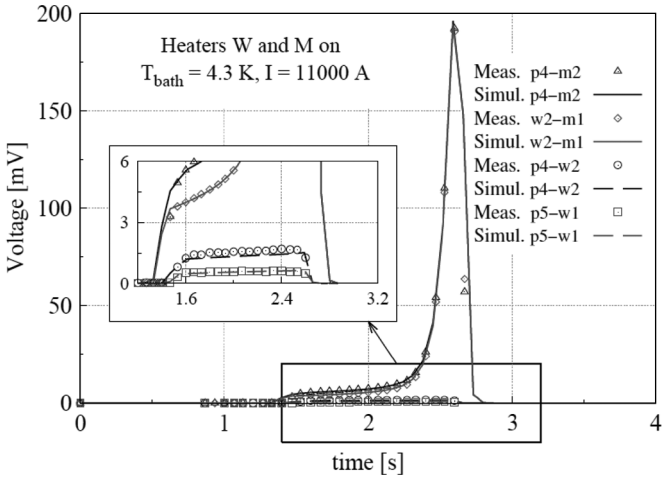

Fig. 7. Measured vs. calculated voltage traces in case of 11 kA current and both heaters switched on.

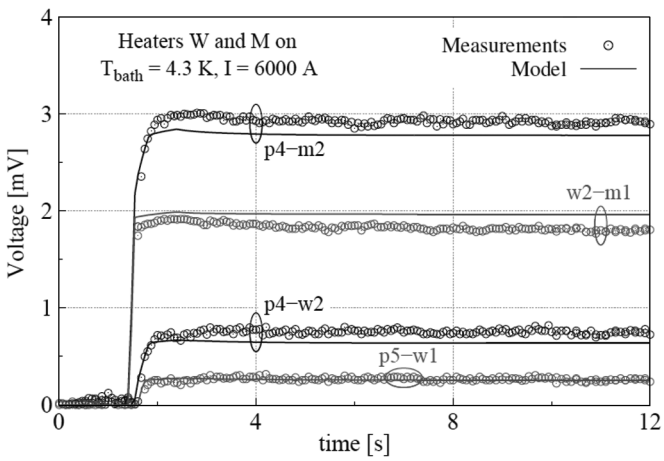

Fig. 8. Measured vs. calculated voltage traces in case of 6 kA current and both heaters switched on.

less efficient heat extraction in the defect zone than in the left side of the IC, thus a hot spot temperature develops.

The computed and experimental voltage traces show very good agreement over the whole measurement. The corresponding temperatures agree as well except for the initial transient state of the U temperature sensor. As previously stated, this agreement could be achieved thanks to the tuning of the transversal thermal and electrical resistances between cables and stabilizer.

Fig. 8 reports the voltages evolution of the same sample in different conditions. In this case the operating current is 6 kA and the pulse lasts between 1 and 2.4 s. The other parameters are identical to the previous test. The voltages start to grow up with a delay of about 0.4 s after the beginning of the heat pulse and they soon reach a steady state value until the end of the measurement, lasting about 50 s. The stabilization is due to the balance between the heat generated in the IC and the heat dissipated towards the helium bath, hence neither propagation nor recovery of the normal zone is observed. Similar agreements between numerical simulations and measurements are found for most of the sample 2B tests in 4.3 K He bath and different transport currents.

V. Conclusion

A thermo-electromagnetic model of the ICs of the 13 kA LHC bus bars was developed, and a thorough numerical analysis of tests reproducing defective ICs was performed. The simulations addressed measurements carried out in 4.3 K He I bath. The modeling approach was based on the definition of local heat transfer coefficients, aiming at obtaining a physical description of the IC underlying thermal and electrical phenomena.

The calculations show good agreement with the measurements. As far as the thermal model is concerned, it highlights that the IC region cannot be considered adiabatic. It also suggests the presence of He in the void spaces inside IC and bus bar, which can explain the observed transient mechanisms. As for the electromagnetic model, it points out the importance of the contact thermal and electrical resistances between SC cables and Cu stabilizer.

Acknowledgment

The authors thank A. P. Verweij, F. Bertinelli, P. Fessia, D. Richter and A. Siemko for the useful discussions.

References

[1] L. Rossi, "Superconductivity: its role, its success and its setbacks in the Large Hadron Collider of CERN," *Superconductor Science and Technology*, vol. 23, pp. 1–17, Feb. 2010.

[2] M. Koratzinos *et al.*, "High-current bus splice resistances and implications for the operating energy of the LHC," in *Proc. of IPAC'10*, Kyoto, 2010, pp. 373–375.

[3] C. Scheuerlein *et al.*, "Production and quality assurance of main busbar interconnection splices during the LHC 2008-2009 shutdown," *IEEE Trans. Appl. Sup.*, vol. 21, pp. 1786–1790, June 2011.

[4] A. P. Verweij, "Minimum requirements for the 13 kA splices for 7 TeV operation," in *Proc. of the Chamonix 2010 Workshop on LHC Performance*, Geneva, 2010, pp. 65–72.

[5] P. P. Granieri, M. Breschi, M. Casali, L. Bottura, and A. Siemko, "Stability analysis of the interconnection of the LHC main superconducting bus bars," *Cryogenics*, submitted for publication.

[6] A. P. Verweij *et al.*, "Consolidation of the 13 kA interconnects in the LHC for operation at 7 TeV," *IEEE Trans. Appl. Sup.*, vol. 21, pp. 2376–2379, June 2011.

[7] G. P. Willering, L. Bottura, P. Fessia, C. Scheuerlein, and A. P. Verweij, "Thermal runaways in LHC interconnections: experiments," *IEEE Trans. Appl. Sup.*, vol. 21, pp. 1781–1785, June 2011.

[8] P. P. Granieri, M. Casali, and D. Richter, "Deat transfer in the LHC main superconducting bus bars," in *Proc. of the 23rd ICEC and ICMC 2010*, Wroclaw, 2010, pp. 411–416.

[9] L. Belova, M. Genet, J.-L. Perinet-Marquet, P. Ivanov, and C. Urpin, "Design and manufacture of the superconducting bus-bars for the LHC main magnets," *IEEE Trans. Appl. Sup.*, vol. 12, pp. 1305–1309, March 2002.

[10] A. Jacquemod, A. Poncet, F. Schauf, B. Skoczen, and J. P. Tock, "Inductive soldering of the junctions of the main superconducing busbars of the LHC," in *LHC Project Report 698, CERN*, Geneva, Switzerland, 2003.

[11] F. Laurent and J. P. Tock, "Modification of the electrical insulation of main bus-bars interconnection," in *LHC Project Document QQBID-EC-0001, CERN*, Geneva, Switzerland, 2009.

[12] L. Bottura, C. Rosso, and M. Breschi, "A general model for thermal, hydraulic, and electric analysis of superconducting cables," *Cryogenics*, vol. 40, pp. 617–626, Dec. 2000.

[13] A. P. Verweij and D. Richter, CERN, private communication, April 2009.

[14] Y. Lei, Y. Yu, Y. Dai, and H. Nan, "Measurements of the interstrand thermal and electrical conductance in multistrand superconducting cables," *IEEE Trans. Appl. Sup.*, vol. 12, pp. 1052–1055, March 2002.